The (Al-Mn) Aluminum-Manganese System

26.98154 54.9380

By A.J. McAlister and J.L. Murray*
National Bureau of Standards

Equilibrium Diagram

Several mutually inconsistent phase diagrams have been proposed to describe the Al-Mn system [Hansen, Elliott, 71God]. Some of the reasons for discrepancies are evident. Mn has been available in high purity only for the last decade or so, it has a high vapor pressure even at relatively high Al-content, and it is readily oxidized. Additionally, more subtle traps have caught many investigators of unquestionable ability. Long-lived metastable phases occur in surprising numbers and reactions leading to the stable equilibria are sluggish. No experiment in this system can be unambiguously interpreted unless the phases are characterized structurally and the approach to equilibrium is demonstrated. Most of the reactions seen during cooling from the liquid state do not pertain to the stable equilibrium diagram at all.

For this reason much of the early work cited by [Hansen] and [Elliott] is considered obsolete and was not used to construct the assessed diagram [e.g., 30Ish, 31Bra, 38Hof, 38Kos]. The major features of the assessed diagram (Fig. 1, Table 1) are based on the present reinterpretation of selected literature results [33Dix, 43Phi, 58Kon, 60Koc, 60Kos, 60Tay, 71God] supported by experimental work at NBS and thermodynamic modeling of stable and metastable equilibria [87Mur].

The following terminology is adopted for the intermetallic compound phases:

- Al_6Mn is firmly established as a stable equilibrium phase [43Ray].
- Two distinct phases, both structurally characterized, have previously been designated "Al_4Mn"; in this evaluation they are distinguished as λ and μ. λ is the phase referred to as Al_4Mn by [60Tay]. The phase that [71God] called Al_4Mn was actually μ [87Mur].
- ϕ ($Al_{10}Mn_3$) is a metastable phase which forms from the liquid during cooling and probably also during decomposition of supersaturated (Al).
- Low- and high-temperature forms of $Al_{11}Mn_4$ are distinguished as $Al_{11}Mn_4$(HT) and $Al_{11}Mn_4$(LT) [71God, 71Abr].
- Three phases in the composition range 30 to 51 at.% Mn, not structurally well characterized, are designated γ, γ_1, and γ_2 after [71God].
- ε is a cph solution phase stable between 53 and 60 at.% Mn and above 870 °C [58Kon, 60Koc].
- τ is a metastable CuAu-type phase that forms martensitically from ε retained during cooling [58Kon].

*Present address: Alcoa Technical Center, Alloy Technology Division, Alcoa Center, PA 15069.

Fig. 1 Assessed Al-Mn Phase Diagram

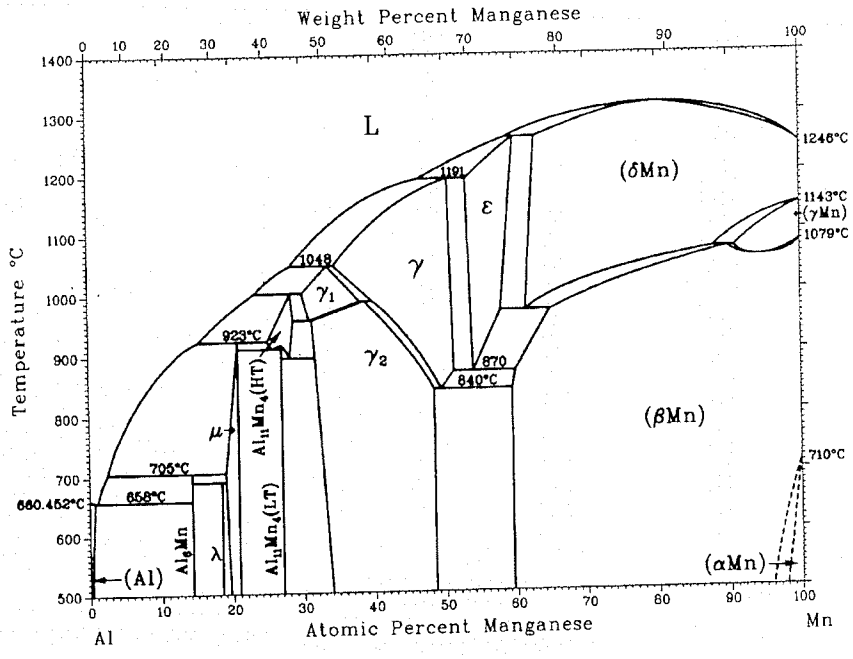

Table 1 Special Points of the Assessed Al-Mn Phase Diagram

Reaction	Compositions of the respective phases, at.% Mn			Temperature, °C	Reaction type
$L \rightleftarrows (Al) + Al_6Mn$	1.0	0.62	14.2	658	Eutectic
$L + \mu \rightleftarrows Al_6Mn$	2.4	19	14.2	705	Peritectic
$L + Al_{11}Mn_4(HT) \rightleftarrows \mu$	15.2	25	20.8	923	Peritectic
$L + \gamma_1 \rightleftarrows Al_{11}Mn_4(HT)$	23.2	30	28.3	1002	Peritectic
$Al_{11}Mn_4(HT) \rightleftarrows \mu + Al_{11}Mn_4(LT)$	25.75	20.8	27	910	Eutectoid
$Al_{11}Mn_4(HT) \rightleftarrows Al_{11}Mn_4(LT)$		27		916	Congruent point
$Al_{11}Mn_4(HT) \rightleftarrows Al_{11}Mn_4(LT) + \gamma_2$	28.2	27	31.8	895	Eutectoid
$L + \gamma \rightleftarrows \gamma_1$	28.3	34.5	33.6	1048	Peritectic
$\gamma_1 \rightleftarrows Al_{11}Mn_4(HT) + \gamma_2$	31	28.7	31.4	957	Eutectoid
$\gamma_1 + \gamma \rightleftarrows \gamma_2$	38.2	40	38.8	1191	Peritectoid
$L + \varepsilon \rightleftarrows \gamma$	43	53.2	50.6	1165	Peritectic
$\gamma \rightleftarrows \gamma_2 + (\beta Mn)$	49.5	47	59.5	840	Eutectoid
$\varepsilon \rightleftarrows \gamma + (\beta Mn)$	54	51.3	60	870	Eutectoid
$L + (\delta Mn) \rightleftarrows \varepsilon$	59	63	60	1260	Peritectic
$(\delta Mn) \rightleftarrows \varepsilon + (\beta Mn)$	61.5	58	65	970	Eutectoid
$L \rightleftarrows (\delta Mn)$		80.3		1315	Congruent point
$(\delta Mn) + (\gamma Mn) \rightleftarrows (\beta Mn)$	87.9	90.9	90	1071	Peritectoid
$(\gamma Mn) \rightleftarrows (\beta Mn)$		94		1055	Congruent point
$L \rightleftarrows (Al)$		0		660.452	Melting point
$L \rightleftarrows (\delta Mn)$		100		1246	Melting point
$(\delta Mn) \rightleftarrows (\gamma Mn)$		100		1143	Allotropic transformation
$(\gamma Mn) \rightleftarrows (\beta Mn)$		100		1079	Allotropic transformation
$(\beta Mn) \rightleftarrows (\alpha Mn)$		100		710	Allotropic transformation

Al-Rich Alloys. The two most recently proposed versions of the Al-rich side of the diagram are from [60Tay] and [71God]. According to [71God], the phases labeled μ and ϕ by [60Tay] do not belong on the equilibrium diagram, and therefore neither do peritectic reactions at 880 and 820 °C. [71God] identified ϕ as a metastable phase that participates in two peritectic reactions, $L + Al_{11}Mn_4(HT) \rightleftarrows \phi$ and $L + \phi \rightleftarrows Al_4Mn$; they did not, however, address the question of the stability of the μ phase. Most of the differences between these two diagrams can be understood in terms of the different experimental techniques that were used.

[60Tay] made an X-ray diffraction (XRD) study of as-cast samples and bulk samples annealed for two weeks at 750, 810, 850, and 950 °C. The diagram was constructed by assuming that all of the observed phases were stable equilibrium phases and assigning melting temperatures to each from the previous thermal analysis work of [33Dix] and [43Phi]. Evidence was obtained that Al_4Mn can persist up to a temperature between 810 and 850 °C, supporting thermal analysis and metallographic results of [43Phi], but no direct evidence was obtained to associate the melting of ϕ with the thermal arrests observed by [33Dix] at ~920 °C. However, the structures of the phases observed by [60Tay] have all been verified by independent studies (including that of μ by [87Mur]).

The investigation by [71God] was carried out using thermal analysis on heating and cooling, supported by metallographic examination but not by XRD. Equilibration times of 80 days, rather than 2 weeks, were used.

Between 12 and 22 at.% Mn, [71God] observed reactions during cooling at about 880, 860, and 840 °C; but on heating equilibrated samples above 800 °C they found only one melting reaction, at 923 °C.

It is concluded that the work of [71God] established the melting reactions of the stable equilibrium diagram, but is not definitive with regard to the identities of the phases in equilibrium. The work of [60Tay] established the structures of phases to be accounted for, but not their stability ranges.

Comparison of the two diagrams suggests three ways in which the diagram proposed by [71God] requires modification:

- All of the phases found by [60Tay] must be included either stably or metastably. That [60Tay] observed no "Al_4Mn" above 810 °C and that [71God] found "Al_4Mn" to be stable up to 923 °C strongly suggests that the phase that [71God] identified as "Al_4Mn" was actually μ. This is consistent with the compositions at which μ and "Al_4Mn" (here called λ) were observed by all investigators [43Phi, 60Tay, 71God].
- The interpretation of the two reactions at 880 and ~860 °C as the metastable peritectic reactions in which ϕ and μ are successively formed from the melt must be revised, because it is not thermodynamically self-consistent. As drawn by [71God], the extension of the ϕ liquidus below 860 °C lies above the (stable) μ liquidus in temperature. Because the metastable two-phase field cannot extend into the stable single-phase liquid field, this construction implies that ϕ is a stable phase. This, however, was not intended by [71God], nor is there any experimental evidence that ϕ is a stable phase.
- There are conflicts about the peritectic temperature at which Al_6Mn is formed. Reactions have been reported at 670 to 690 °C (on cooling) and at about 710 °C (on heating). It is usually assumed that the lower reaction is the effect of undercooling and involves the same phases as the higher reaction. Thus, most investigators [43Phi, 60Tay, 71God] placed the equilibrium peritectic isotherm between 700 and 710 °C. However, [43Phi] disputed this interpretation: he found arrests at 690 °C on both heating and cooling, but none at 710 °C. When the λ phase is incorporated into the diagram, it is plausible to suppose that Al_6Mn may be formed from either $L + \mu$ or $L + \lambda$ and that the two reactions may occur near 700 °C.

Fig. 2 Al-Rich Part of Al-Mn Diagram vs Thermal Analysis Data (Heating)

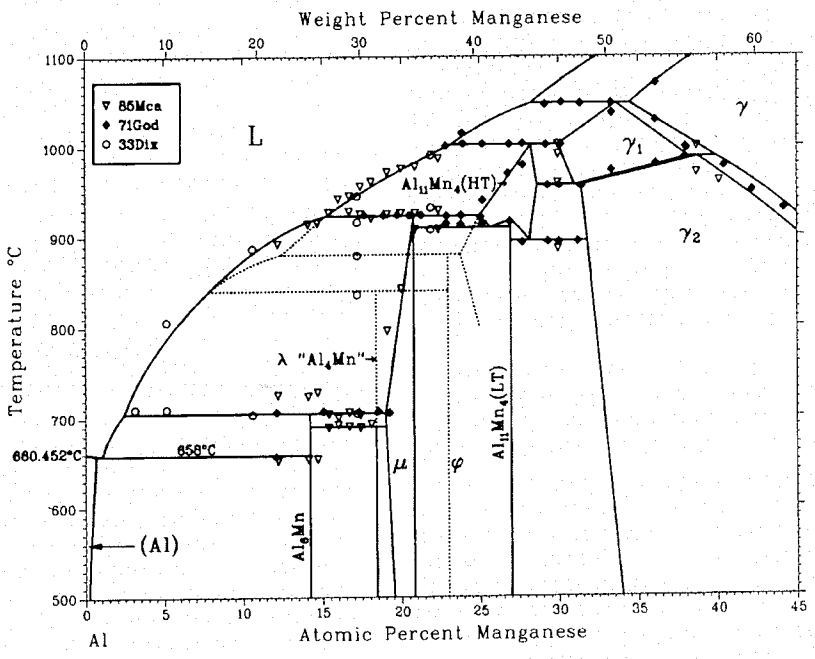

——— = stable equilibria; ····· = metastable equilibria.

A.J. McAlister and J.L. Murray, 1987.

Fig. 3 Al-Rich Part of Al-Mn Diagram vs Thermal Analysis Data (Cooling)

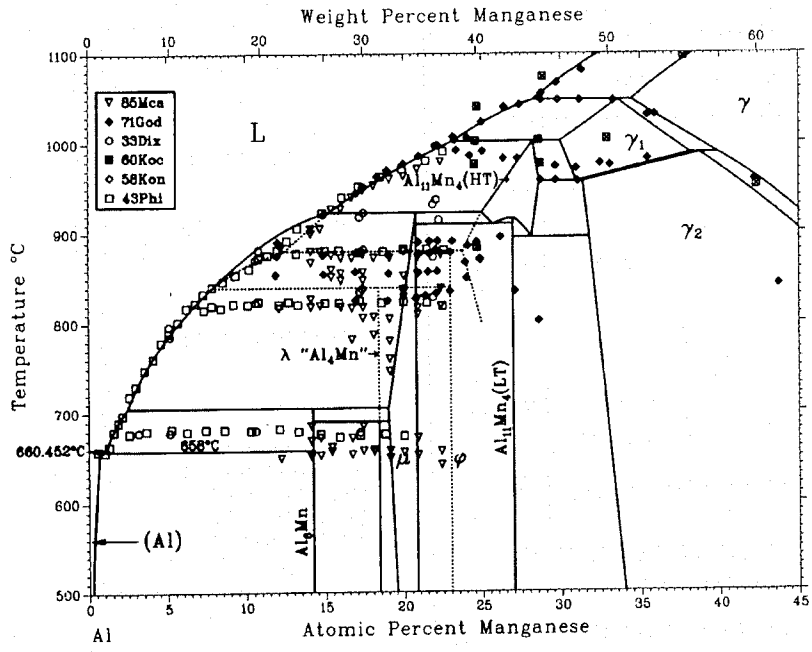

——— = stable equilibria; ····· = metastable equilibria.

A.J. McAlister and J.L. Murray, 1987.

Table 2 Solid Solubility of Mn in (Al)

Reference	(Al) solvus composition, at.% Mn	Temperature, °C	Method
[40Fah]	0.22	500	Electrical resistivity
	0.29	550	(equilibrated and
	0.48	600	quenched samples)
[45But]	0.168	500	Optical microscopy
	0.385	591	(selected)
	0.524	630	
	0.560	640	
	0.605	649	
	0.621	654	
[53Obi]	0.06	447	Lattice parameter
	0.150	500	
	0.309	550	
	0.512	600	
	0.710	633	
[33Dix]	0.199	500	Optical microscopy
	0.388	570	
	0.681	630	
[64Dri]	0.302	620	Optical microscopy
	0.222	600	
	0.099	500	
	0.078	350	
	0.226	600	Electrical resistivity
	0.113	500	

Fig. 4 Solubility of Mn in (Al)

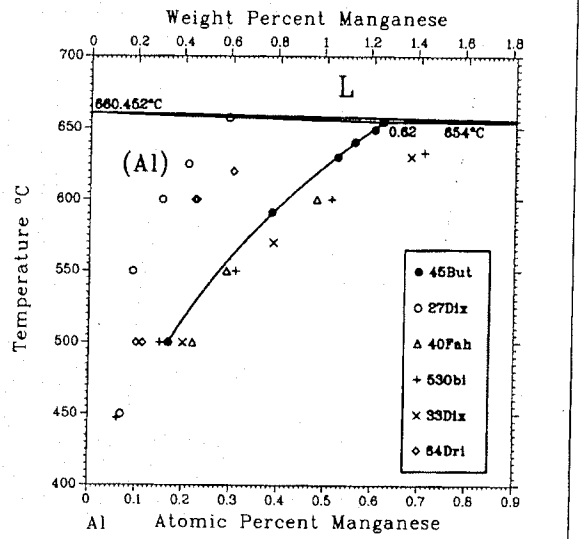

A.J. McAlister and J.L. Murray, 1987.

The experimental techniques used by [87Mur] were constant heating/cooling rate differential thermal analysis (DTA), XRD, and transmission electron microscopy (TEM). The samples studied were splat-quenched ribbons containing from 12 to 55 at.% Mn, prepared from 99.999 at.% Al and 99.98 at.% Mn.

In the as-quenched condition, almost all of the samples contained metastable phases. The approach to equilibrium of the metastable samples under constant heating rate conditions was studied to assure the relevance of higher-temperature DTA results to the equilibrium diagram. After the equilibrium phase assemblage was obtained, subsequent transformations occurred at temperatures in excellent agreement with those reported by [71God] in heating of samples heat treated for 80 days at 700 °C. All of the samples in the 12.2 to 22.4 at.% Mn range were also cooled from the liquid. In addition to the liquidus and invariant melting reactions, [87Mur] confirmed the $\gamma_1 \rightleftarrows Al_{11}Mn_4(HT) + \gamma_2$ eutectoid at 957 °C and the $\gamma_1 + \gamma_1 \rightleftarrows \gamma_2$ peritectoid at 900 °C reported by [71God]. The only discrepancies between [71God] and [87Mur] are in the neighborhood of 700 °C. [71God] identified the room temperature equilibrium phase at 20 at.% Mn as "Al_4Mn" (λ phase), evidently without performing XRD structural analysis. It is clear from the XRD results that the low-temperature equilibrium phase at 20 at.% is μ [87Mur].

This leaves the question of how to incorporate λ in the stable or metastable phase diagram, between Al_6Mn and μ. [87Mur] presented evidence from melting studies that λ is a stable equilibrium phase, formed in the peritectoid reaction $Al_6Mn + \mu \rightleftarrows \lambda$ at 693 ± 2 °C, and that λ is single phase at 18 at.% Mn and 680 °C. The stable equilibrium peritectic reaction $L + \mu \rightleftarrows Al_6Mn$ occurs at 706 ± 3 °C.

Thermal analysis data (heating) are compared with the assessed diagram in Fig. 2; cooling data are superimposed on the calculated stable and metastable diagram in Fig. 3. The assumptions on which the calculation is based and its use in the interpretation of the cooling data are discussed in detail below.

(Al) Solvus, Solidus, and Liquidus. The solubility of Mn in (Al) was investigated by [27Dix], [33Dix], [40Fah], [45But], [53Obi], and [64Dri]. The data are summarized in Table 2 and compared with the assessed solvus in Fig. 4. The results of [27Dix] can be discounted because of the effect of impurities; the results of [64Dri] were probably also influenced by contamination. The discrepancy between [53Obi] and [45But] cannot be resolved by consideration of impurity levels or failure to reach equilibrium. The results of [45But] are used to construct the assessed diagram because of their consistency with a series of investigations of ternary and quaternary alloys and the good fit of six $\ln x$ vs $1/T$ data points to a straight line. The maximum solubility is 0.62 at.% Mn at 658 °C.

The eutectic reaction $L \rightleftarrows (Al) + Al_6Mn$ occurs at 658 ± 1 °C and the eutectic composition is 1.0 ± 0.1 at.% Mn [33Dix, 43Phi]. These values are consistent with the thermodynamic properties of pure Al.

cph ε is a solution phase stable between 53.2 and 60 at.% Mn and between the solidus and the eutectoid reaction $\varepsilon \rightleftarrows \gamma_2 + (\beta Mn)$ at 870 °C. This phase was first observed by [58Kon], who identified two reactions, $\varepsilon \rightleftarrows \gamma + (\beta Mn)$ at 870 °C and $\gamma \rightleftarrows \gamma_2 + (\beta Mn)$ at 840 °C, by specific heat measurements. The eutectoid compositions were estimated as 50 and 55 at.% Mn, respectively, the compositions at which the heats of the eutectoid reactions reached their maxima. [58Kon] also made metallographic and thermal analysis determinations of the $\varepsilon + (\beta Mn)$, $\varepsilon + \gamma$, and $\gamma_2 + (\beta Mn)$ two-phase fields up to 1000 °C. The structure and stability of ε were verified by [60Koc] (by thermal analysis and XRD) and [60Kos] (by magnetic and hardness measurements, XRD, and metallography). [60Koc] verified the thermal analysis results of [58Kon], placing the eutectoid reactions at 850 and 870 °C. [60Kos] found invariant reactions at 800, 840, and 870 °C, and interpreted them somewhat differently from [58Kon]. The eutectoid reaction $\gamma \rightleftarrows \gamma_2 + (\beta Mn)$ was placed at 800 °C,

Fig. 5 Mn-Rich Part of Al-Mn Diagram with Select Experimental Data

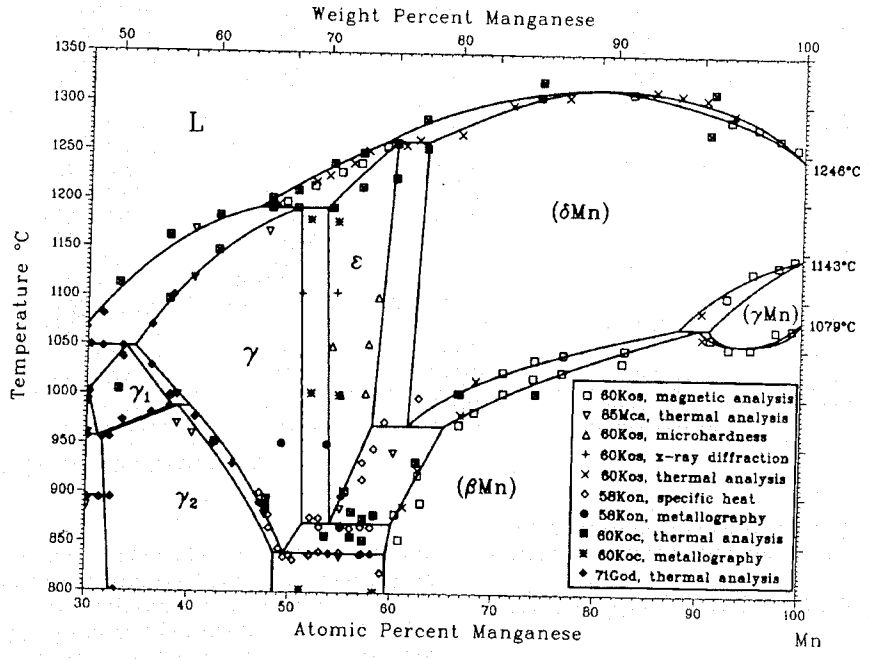

A.J. McAlister and J.L. Murray, 1987.

and the isotherm at 840 °C was interpreted as the reaction (δMn) ⇄ γ + (βMn). The diagram of [Elliott] was based on [60Kos]. However, that interpretation left unexplained the metallographic and XRD data of [58Kon]; moreover, later work from the same laboratory [71God] confirmed the [58Kon] work rather than the [60Kos] results. Therefore, the (δMn) ⇄ (βMn) + ε reaction is placed at 955 °C and the 840 °C reaction is interpreted as γ ⇄ γ2 + (βMn). This is consistent with the combined experimental data, as shown in Fig. 5.

(Mn) Solid Solutions. The solubility of Al in bcc (δMn) and (βMn) is known to be high (~ 40 at.% in each), as can be seen from the data plotted in Fig. 5. The (δMn) liquidus is based on thermal and magnetic analysis [60Koc] and is qualitatively confirmed by thermal analysis results of [60Kos]. For the (γMn) boundaries, however, only scattered magnetic data [60Kos] are available. These data have previously been interpreted as follows: addition of Al lowers both the (δMn) ⇄ (γMn) and (γMn) ⇄ (βMn) transformation temperatures, and the (γMn) field terminates at a eutectoid reaction (γMn) ⇄ (δMn) + (βMn) [Hultgren, B; Elliott; 60Kos, 71God]. However, these diagrams [e.g., Elliott] violate fundamental thermodynamic constraints on metastable extensions of the phase boundaries. Moreover, the metastable βMn → δMn transition in pure Mn must occur above the βMn ⇄ γMn transformation and below the δMn ⇄ γMn transformation; the diagrams of [60Kos] and [Elliott] also violate this constraint. The assessed invariant reaction of (δMn), (γMn), and (βMn) is therefore drawn as a peritectoid reaction, (δMn) + (γMn) ⇄ (βMn), with a congruent transformation (γMn) ⇄ (βMn). The minimum in the (γMn) ⇄ (βMn) boundaries actually fits the experimental data somewhat better than previous constructions.

The (αMn)/(βMn) equilibria were examined only cursorily by [60Kos] using magnetic analysis. Addition of Al stabilizes (βMn) relative to (αMn) and the solubility of Al in (αMn) is probably quite low.

Metastable Phases

Quasicrystals. The quasicrystalline state is characterized by long-range orientational order of five-fold symmetry, but no translational invariance. The quasicrystalline phase was discovered by [84She1] and [84She2] in a melt-spun sample containing 14 at.% Mn. The point group symmetry is $m\bar{3}5$ (the symmetry of the icosahedron); the structure is that of an aperiodic tiling [85Por] which is characterized by scaling invariance under multiplication by the golden ratio $\tau = (\sqrt{5} + 1)/2 = 1.6803$. By high-resolution electron microscopy, it has been shown that the unusual diffraction pattern of the quasicrystals is not explained by microtwinning (as proposed by [84Fie]) or by incommensurate modulated structures.

The icosahedral phase is formed from the metastable liquid by a first order transition, with separation of fcc (Al). The composition of the icosahedral phase is about 20 at.% Mn [85Guy, 85Kim, 86Sch]. The heat of transformation to Al_6Mn is 2 kJ/mol [85Kel, 87Mca].

At somewhat higher Mn content, another quasicrystalline phase (decagonal or T phase) is formed in melt-spun ribbons. It has a 10-fold symmetry axis and one dimensional translational periodicity along this axis [85Ben, 86Ben, 86Sch].

On heating, the quasicrystalline phases transform to the equilibrium phase assemblages by often complex processes, which were partially mapped out by [87Mur].

Many papers have recently appeared on the local atomic structure and diffraction theory of the quasicrystalline phases. Treatment of this rapidly developing field is beyond the scope of this review.

Decomposition of Supersaturated (Al). By rapid solidification the solubility of Mn in (Al) can be extended beyond the equilibrium value of 0.62 at.% Mn [52Fal, 56Fri, 65Bur, 69Mir, 70Ble, 70Hin, 72Nes]. The solubilities achieved by the most rapid quenching techniques (>10^5 °C/s) are about 6 to 6.7 at.% Mn [69Mir, 70Ble]; cooling rates of the order of 10^4/°C range from 1.8 to 4 at.% Mn [52Fal, 65Bur, 70Hin].

The decomposition of the supersaturated solid solution proceeds via the formation of a number of metastable phases, most of them usually designated G phases. Because of nonuniformity of nomenclature the phases are best described by their crystal structures:

- A phase (the original "G-phase") of simple cubic structure with a = 1.328 nm [47Lit, 48Lit]. According to [72Nes] this phase is stabilized by impurities.
- A phase with the bcc $Al_{12}W$ structure [47Mar] and lattice parameter a = 0.7533 nm [74Goe] or 0.754 nm [72Nes], or a = 0.7507 [54Ada]. This phase is now usually designated G (see "Crystal Structures").
- A simple cubic structure similar to that of $\alpha Al_{12}Mn_3Si$ [72Nes].
- An orthorhombic Al_7Cr-type phase with a = 0.251, b = 2.48, and c = 3.03 nm [74Goe].
- A hexagonal phase with a = 0.754 nm and c = 0.784 nm [72Nes, 84She1]. The lattice parameters of this precipitate are close to those reported for $Al_{10}Mn_3$ (ϕ).
- After short anneals in the temperature range 560 to 600 °C [73Hoi] found a trigonal phase with a = 2.86 nm and α = 36.0°.

The $Al_{12}W$-type G phase is very close to being a stable phase of the system; initially in supersaturated (Al), it grows at the expense of Al_6Mn [84She1].

Ferromagnetic τ Phase. The high-temperature cph ε phase transforms to a metastable ferromagnetic phase τ (with the $L1_0$ CuAu structure) during cooling from the ε region at rates of about 10 °C/s [58Kon, 60Koc] or during tempering of retained ε at low temperatures (~325 to 350 °C) [60Kos, 67Mag]. The metastability of τ was shown by the formation of two-phase assemblages of (βMn) + γ_2 during slow cooling or prolonged isothermal treatment [58Kon, 60Koc]. τ appears to be an equilibrium phase at pressures above 60 kbar [65Ern].

The τ phase is of interest as a material for permanent magnets because of its high magnetic anisotropy. Magnetic properties were examined by [58Kon], [60Koc], [60Kos], and [67Mag]. The Curie temperature, T_C, was reported as 365 °C [60Kos], 373 °C [58Kon], and 380 °C [60Koc].

[60Kos] reported temperatures of both the start and finish of the $\varepsilon \rightleftarrows \tau$ transformation as a function of cooling rate. For rates below about 6 °C/s the product of the transformation was equilibrium (βMn) + γ_2; for rates between about 6 and 15 °C/s, the transformation $\varepsilon \rightleftarrows \tau$ started at ~710 °C; at higher rates, ε was retained after cooling. [58Kon] also found that a 55.1 at.% Mn sample started to transform at about 730 °C for cooling rates near 10 °C/s. [60Koc] reported that τ was formed at somewhat higher cooling rates, ~30 °C/s.

According to [73Vin], based on X-ray and neutron diffraction, the $\varepsilon \rightarrow \tau$ transition occurs via the formation of an intermediate ordered hexagonal AuCd-type structure.

Crystal Structures and Lattice Parameters

Crystal structure data for equilibrium and metastable phases are summarized in Table 3. Lattice parameters of

Table 3 Al-Mn Crystal Structure Data

Phase	Composition, at.% Mn	Pearson symbol	Space group	Strukturbericht designation	Prototype	Reference
(Al)	0 to 0.62	*cF*4	$Fm\bar{3}m$	*A*1	Cu	[Pearson2]
G(a)	(b)	*cI*26	$Im\bar{3}$	...	$Al_{12}W$	[54Ada]
Al_6Mn	14.2	*oC*28	*Cmcm*	$D2_h$	Al_6Mn	[53Nic, 80Kon]
λ("Al_4Mn") (c)	~16.8 to 19	Hexagonal	...	...	...	...
μ	~19 to 20.8	Hexagonal	...	...	...	...
φ($Al_{10}Mn_3$)	(b)	*hP*28	$P6_3/mmc$	$D8_{11}$	Co_2Al_5	[60Tay]
$Al_{11}Mn_4$(LT) (d)	27	*aP*30	$P\bar{1}$	...	...	[58Bla, 60Tay]
$Al_{11}Mn_4$(HT) (d)	25 to 28.7	*oP*160	*Pnma*	...	...	[71Abr, 61Tay]
γ_1	30 to 38.2	Unknown	...	...	...	...
γ_2(e)	31.4 to 47	*hR*26	$R\bar{3}m$	$D8_{10}$	Cr_5Al_8	[69Sch]
γ(f)	34.5 to 51.3	Unknown	...	...	...	...
ε	53.2 to 60	*hP*2	$P6_3/mmc$	*A*3	Mg	[58Kon]
τ	(b)	*tP*2	$P4/mmm$	$L1_0$	CuAu	[58Kon]
(δMn)	61.5 to 100	*cI*2	$Im\bar{3}m$	*A*2	W	[Pearson2]
(γMn)	90.9 to 100	*cF*4	$Fm\bar{3}m$	*A*1	Cu	[Pearson2]
(βMn)	59.5 to 100	*cP*20	$P4_132$	*A*13	βMn	[Pearson2]
(αMn)	~98 to 100	*cI*58	$I\bar{4}3m$	*A*12	αMn	[Pearson2]

(a) A number of other structures have been ascribed to G phase or variants of G phase (G', G"). See "Metastable Phases". (b) Metastable phase. (c) [75Oni] found a simple orthorhombic structure with a = 0.6795 nm, b = 0.9343 nm and c = 1.3897 nm in an alloy described as "Al_4Mn". (d) Variants of this structure are described as complex stacking sequences along the b axis [73Yos, 72Yos]. Lattice parameters of $Al_{11}Mn_4$(LT) are a = 0.5095(4) nm, b = 0.8879(8) nm, c = 0.5051(4) nm, α = 89.35(7)°, β = 100.47(5)°, γ = 105.08(6)°. (e) The structure has been described as distorted γ-brass type [60Kos], cubic (bcc or fcc) [65Ern], and rhombohedral [60Koc, 60Sch, 69Sch, 71Yos]. The descriptions by [60Sch], [69Sch], and [71Yos] can all be reduced to the Al_8Cr_5 structure given by [60Sch]. (f) [65Ern] reported a bcc and an fcc structure, one of which belonged to the γ phase.

hexagonal phases, of orthorhombic phases, and of ε and τ are listed in Table 4. Lattice parameters of supersaturated (Al) solid solution are plotted in Fig. 6. Icosahedral and decagonal quasi-crystalline phases are described above ("Metastable Phases"), as are various metastable precipitates from supersaturated (Al).

Fig. 6 Lattice Parameters of Supersaturated (Al)

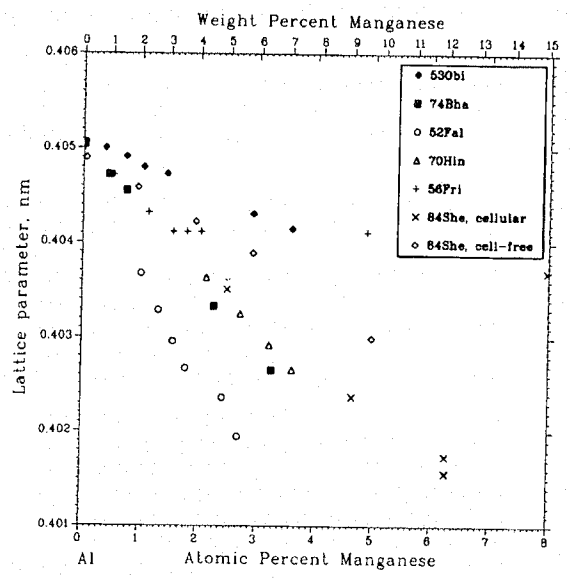

A.J. McAlister and J.L. Murray, 1987.

Thermodynamics

The aim of the present calculations is to construct Gibbs energy functions for the liquid, fcc, Al_6Mn, λ, μ, ϕ, and $Al_{11}Mn_4$ phases which reproduce the stable liquidus, invariant reactions, and thermochemical data and predict the metastable phase equilibria.

Gibbs energies of the compounds Al_6Mn, λ, μ, $Al_{10}Mn_3(\phi)$, and $Al_{11}Mn_4$ are represented in the form $G^0 = H^0 - TS^0$; that is, for the purpose of the present calculations the homogeneity ranges and heat capacity differences need not be taken into account. (For simplicity, the transformation from high to low $Al_{11}Mn_4$ forms is ignored.)

Excess Gibbs energies of the liquid, fcc, bcc, and (βMn) solution phases are represented as polynomial expansions.

$$G^{ex} = x_{Al}x_{Mn}\,[A(T) + B(T)\,(x_{Al} - x_{Mn}) + \Sigma\, C_i(T)\,P_i(x_{Al} - x_{Mn})]$$

where x_{Al} and x_{Mn} are atomic fractions of Al and Mn; P_i are Legendre polynomials; and A, B, and C are temperature dependent coefficients of the polynomial expansion.

The number of coefficients used to describe each solution phase was chosen in each case as the fewest required to fit the selected experimental data within the estimated experimental uncertainty. Thermodynamic data for the liquid come from different experimental techniques and have different accuracy over the composition range. Enthalpies of mixing were measured calorimetrically over the whole range by [73Esi]; the enthalpies have not yet been verified by an independent investigation. They reach a minimum of −17 000 J/mol and are reproduced by a subregular solution model with maximum discrepancy of 600 J/mol. The excess entropy is derived from partial Gibbs energies measured by the emf technique by [72Bat]. The data were assessed by [85Des]: the assessed integral

Table 4 Al-Mn Lattice Parameter Data

Phase	Composition, at.% Mn	Lattice parameters, nm a	b	c	Reference
Hexagonal phases					
$\phi(Al_{10}Mn_3)$	~23	0.7543	...	0.7898	[60Tay]
λ	~17	2.84	...	1.24	[60Tay]
		2.835	...	1.236	[38Hof]
μ	~20	1.995	...	2.452	[60Tay]
γ_2	42	1.2739	...	1.5861	[60Sch]
		1.2630	...	1.5866	[69Sch]
Orthorhombic phase					
Al_6Mn	14.3	0.75551	0.64994	0.88724	[80Kon]
		0.755	0.650	0.887	[60Tay]
		0.75518	0.64978	0.88703	[53Nic]
		0.757	0.651	0.887	[38Hof]
		0.757	0.650	0.889	[53Sch]
		0.7564	0.6500	0.8883	[75Oni]
ε and τ phases (a)					
ε	55.1	0.269	...	0.438	[58Kon]
	55.5	0.2697	...	0.4356	[60Kos]
	55.8	0.2705	...	0.4361	[67Mag]
τ	55.1	0.279	...	0.358	[58Kon]
	55.5	0.277	...	0.357	[60Koc]
	55.5	0.277	...	0.354	[63Bra]
	55.8	0.278	...	0.356	[67Mag]

Note: At room temperature.
(a) For the CuAu structure a larger unit cell ($tP4$) is sometimes used. All a parameters are converted to the standard ($tP2$) unit cell.

excess entropies S^{ex} are negative at the Al-rich end but positive at the Mn-rich end; they reach a minimum of −5.403 J/mol · K at $x_{Mn} = 0.4$, with an assessed uncertainty of ±2.5 J/mol · K. It is therefore not clear that even the variation from positive to negative S^{ex} is real, and S^{ex} is represented by one symmetrical term in the polynomial expansion.

The liquid phase Gibbs energy was checked for consistency with the phase diagram over the whole range. At intermediate compositions, accurate calculation of the diagram is ruled out by lack of information about the structures of several phases whose homogeneity ranges are substantial and whose Gibbs energies would be required in some detail. However, it has been verified that the phase equilibria among the liquid and the bcc, fcc, and (βMn) solid solutions can be calculated starting with the subregular solution model for the liquid and estimated regular and subregular contributions to the solid phase Gibbs energies.

[60Kub] measured enthalpies of formation of alloys containing 14.2, 20, and 26.7 at.% Mn by direct reaction calorimetry at 300 to 350 °C. They estimated that the results were accurate to ±1000 J/mol and reported that completeness of alloy formation was verified by XRD and metallographic analysis. It can be assumed that the 14.2 and 26.7 at.% Mn alloys had formed stable Al_6Mn and $Al_{11}Mn_4$(LT) respectively; however, in view of the even recent failure to distinguish λ and μ, it is not clear what phases were present in the 20 at.% Mn alloy. Therefore, the enthalpies of Al_6Mn and $Al_{11}Mn_4$ are based on data from [60Kub]; the enthalpies of λ, μ, and ϕ have been estimated as approximately equal to those of Al_6Mn and $Al_{11}Mn_4$ and adjusted to fulfill the requirement that above about 400 °C, ϕ is a metastable phase. The range 0 to 30 at.% Mn was calculated. The following assumptions were made for the calculation of the range 0 to 30 at.% Mn:

- The liquidus between 923 and 990 °C is that of $Al_{11}Mn_4$, and the peritectic reaction at 923 °C is $L + Al_{11}Mn_4 \rightleftarrows \mu$.
- At about 700 °C two peritectic reactions compete for stability, $L + \mu \rightleftarrows Al_6Mn$ and $L + \lambda \rightleftarrows Al_6Mn$.
- The peritectic reaction at 880 °C is $L + Al_{11}Mn_4 \rightleftarrows \phi$ and it is metastable.
- If μ is not considered, then λ is the next most stable phase, in equilibrium with the liquid up to about 800 to 830 °C.

These assumptions were sufficient to estimate the entropies of fusion of Al_6Mn and $Al_{11}Mn_4$ and the Gibbs energies of μ, λ, and ϕ. The Gibbs energy parameters are listed in Table 5.

Discussion and Calculations. In Fig. 3, six liquidus curves are shown: those representing equilibrium with fcc Al, Al_6Mn, λ, μ, ϕ, and $Al_{11}Mn_4$. The stable liquidus (the uppermost curve) consists of branches for $Al_{11}Mn_4$, μ, and Al_6Mn. The calculated stable equilibrium invariant reactions are:

$L + Al_{11}Mn_4 \rightleftarrows \mu$ at 924 °C

$L + \mu \rightarrow Al_6Mn$ at 705 °C

$\mu + Al_6Mn \rightleftarrows \lambda$ at 693 °C

Other points where one liquidus branch crosses another give rise to metastable peritectic reactions that can be observed experimentally when the more stable phases cannot nucleate and grow. A metastable equilibrium diagram can be obtained by imposing the constraint that a particular phase does not appear. In Al-Mn the appropriate phase to omit is μ, and the metastable sequence of peritectic reactions is:

$L + Al_{11}Mn_4 \rightarrow \phi$ at 884 °C

$L + \phi \rightarrow \lambda$ at 847 °C

$L + \lambda \rightarrow Al_6Mn$ at 715 °C

Experimentally, the reaction $L + Al_{11}Mn_4 \rightarrow \phi$ is the most reproducible of the peritectic reactions seen on cooling. The lower peritectic reactions are predicted to be the only ones to occur during cooling if each succeeding reaction proceeds to completion. However, in this system reactions are not completed during slow cooling. If it is assumed that all solid phases formed at high temperature are present (for example $Al_{11}Mn_4$ below 884 or ϕ below 847 °C), then there are additional peritectic reactions by which they can decompose to more stable assemblages:

$L + Al_{11}Mn_4 \rightarrow \lambda$ at 858 °C

$L + Al_{11}Mn_4 \rightarrow Al_6Mn$ at 831 °C

$L + \phi \rightarrow Al_6Mn$ at 818 °C

In some cooling curves as many as five distinct reactions have been observed between 800 and 900 °C, and the present calculation should be understood as a predictive guide to identifying the phases in equilibrium in the sequence of reactions.

Cited References

***27Dix:** E.H. Dix and W.D. Keith, "Equilibrium Relations in Aluminum-Manganese Alloys of High Purity," Proc. AIME, Inst. Metals Div., 315-335 (1927). (Equi Diagram; Experimental)

30Ish: T. Ishiwara, "On the Equilibrium Diagrams of the Aluminum-Manganese, Copper-Manganese and Iron-Manganese Systems," *Sci. Rep. Tohoku Univ., 19*, 499-511 (1930). (Equi Diagram; Experimental)

31Bra: A.J. Bradley and P. Jones, "The Aluminum-Manganese System of Alloys," *Philos. Mag., 12*, 1137-1152 (1931). (Crys Structure; Experimental)

Table 5 Al-Mn Thermodynamic Properties

Gibbs energies of the pure components

$G(L, Mn) = 0$
$G(L, Al) = 0$
$G(bcc, Mn) = -14\,644 + 9.6395T$
$G(bcc, Al) = -627.6 + 6.6944T$
$G(fcc, Mn) = -16\,401 + 10.8803T$
$G(fcc, Al) = -10\,711 + 11.473T$
$G(Al_6Mn) = -27\,215 + 14.95T$
$G(\lambda) = -31\,518 + 17.0988T$
$G(\mu) = -34\,951 + 17.8T$
$G(\phi) = -35\,400 + 17.025T$
$G(Al_{11}Mn_4) = -35\,250 + 15.1T$

Parameters for excess Gibbs energies of solution phases

$A(L) = -68\,000 + 17T$
$B(L) = -8\,000$
$A(bcc) = -84\,000 + 16T$
$B(bcc) = -11\,000$
$A(fcc) = -67\,950 + 16T$
$B(fcc) = 3\,500$

Note: Values are in J/mol and J/mol · K.

*33Dix: E.H. Dix, W.L. Fink, and L.A. Willey, "Equilibrium Relations in Aluminum-Manganese Alloys of High Purity, II," *Trans. AIME, 104*, 335-352 (1933). (Equi Diagram; Experimental)

38Hof: W. Hofmann, "Roentgenographic Methods in the Investigation of Aluminum Alloys," *Aluminium, 20*, 865-872 (1938). (Crys Structure; Experimental)

*38Kos: W. Koster and W. Bechthold, "The Manganese-Aluminum System," *Z. Metallkd., 30*, 294-296 (1938). (Equi Diagram; Experimental)

40Fah: E. Fahrenhorst and W. Hofmann, "The Solubility of Manganese in Aluminum Containing up to 2 Percent Magnesium," *Metallwirtschaft, 19*, 891-893 (1940). (Equi Diagram; Experimental)

*43Phi: H.W.L. Phillips, "The Constitution of Alloys of Aluminum with Manganese, Silicon, and Iron. I.—The Binary System: Aluminum-Manganese. II.—The Ternary Systems: Aluminum-Manganese-Silicon and Aluminum-Manganese-Iron," *J. Inst. Met., 69*, 275-350 (1943). (Equi Diagram; Experimental)

43Ray: G.V. Raynor and W. Hume-Rothery, "The Constitution of Magnesium-Manganese-Zinc-Aluminum Alloys in the Range 0-5 Percent Magnesium, 0-2 Percent Manganese, 0-8 Percent Zinc. II—The Composition of The $MnAl_6$ Phase," *J. Inst. Met., 69*, 415-421 (1943). (Equi Diagram; Experimental)

*45But: E. Butchers and W. Hume-Rothery, "The Solubility of Manganese in Aluminum," *J. Inst. Met., 71*, 87-91 (1945). (Equi Diagram; Experimental)

47Lit: K. Little, G.V. Raynor, and W. Hume-Rothery, "A New Aluminum-Rich Phase in the Alloys of Aluminum and Manganese," *J. Inst. Met., 73*, 83-90 (1947). (Meta Phases; Experimental)

47Mar: G. Marchand, correspondence on Miss K. Little, Dr. G.V. Raynor, and Dr. W. Hume-Rothery's Paper: "A New Aluminum-Rich Phase in the Alloys of Aluminum and Manganese," *J. Inst. Met., 71*, 747-749 (1947). (Meta Phases; Experimental)

48Lit: K. Little and W. Hume-Rothery, "A Note on the Aluminum-Manganese G Phase," *J. Inst. Met.*, 521-525 (1948). (Meta Phases; Experimental)

52Fal: G. Falkenhagen and W. Hofmann, "Influence of High Cooling Rates on Solidification and Structure of Binary Alloys," *Z. Metallkd., 43*, 69-81 (1952) in German. (Meta Phases; Experimental)

53Nic: A.D.I. Nicol, "The Structure of $MnAl_6$," *Acta Crystallogr., 6*, 285-293 (1953). (Crys Structure; Experimental)

53Obi: I. Obinata, E. Hata, and K. Yamaji, "Chiefly on the Sub-Cooled Aluminum-Manganese Alloys," *Jpn. J. Inst. Met., 17*, 496-501 (1953). (Equi Diagram; Experimental)

53Sch: K. Schubert and M. Kluge, "The Bond Character of Fe_2Al_5 and $MnAl_6$," *Z. Naturforsch. A, 8*, 755-756 (1953). (Crys Structure; Experimental)

54Ada: J. Adam and J.B. Rich, "The Crystal Structure of WAL_{12}, $MoAl_{12}$, and $(Mn,Cr)Al_{12}$," *Acta Crystallogr., 7*, 813-816 (1954). (Crys Structure; Experimental)

56Fri: I.N. Fridlyander, V.A. Konstantinov, and N.I. Zaitseva, "The Lattice Parameters of Aluminum-Manganese Alloys After Different Types of Thermal Treatment," *Zh. Fiz. Khim., 30*(7), 1623-1625 (1956) in Russian. (Meta Phases; Experimental)

58Bla: J.A. Bland, "Studies of Aluminum-Rich Alloys with the Transition Metals Manganese and Tungsten. II. The Crystal Structure of (Mn-Al)-Mn_4Al_{11}," *Acta Crystallogr., 11*, 236-244 (1958). (Crys Structure; Experimental)

*58Kon: H. Kono, "On the Ferromagnetic Phase in Manganese-Aluminum System," *J. Phys. Soc. Jpn., 13*(12), 1444-1451 (1958). (Equi Diagram; Experimental)

*60Koc: A.J.J. Koch, P. Hokkeling, M.G.v.d. Steeg, and K.J. De Vos, "New Material for Permanent Magnets on a Base of Mn and Al," *J. Appl. Phys., 31*(5), 75S-77S (1960). (Equi Diagram; Experimental)

*60Kos: W. Koster and E. Wachtel, "Magnetic Investigation of Aluminium-Manganese Alloys Containing More than 25 at.% Mn," *Z. Metallkd., 51*, 271-280 (1960). (Equi Diagram; Experimental)

60Kub: O. Kubaschewski and G. Heymer, "Heats of Formation of Transition-Metal Aluminides," *Trans. Faraday Soc., 56*, 473-478 (1960). (Thermo; Experimental)

60Sch: K. Schubert, S. Bhan, W. Burkhardt, R. Gohle, H.G. Meissner, M. Potzschke, and E. Stolz, "The Structure of Metallic Phases," *Naturwissenschaften, 47*, 303 (1960). (Crys Structure; Experimental)

*60Tay: M.A. Taylor, "Intermetallic Phases in the Aluminum-Manganese Binary System," *Acta Metall., 8*, 256-262 (1960). (Equi Diagram, Crys Structure; Experimental)

61Tay: M.A. Taylor, "The Space Group of $MnAl_3$," *Acta Crystallogr., 14*, 84 (1961). (Crys Structure; Experimental)

63Bra: P.B. Braun and J.A. Goedkoop, "An X-Ray and Neutron-Diffraction Investigation of the Magnetic Phase $Al_{0.89}Mn_{1.11}$," *Acta Crystallogr., 16*, 737-740 (1963). (Crys Structure; Experimental)

64Dri: M.E. Drits, E.S. Kadaner, E.M. Padezhnova, and N.R. Bochvar, "Determination of the Boundaries of Common Solubility of Manganese and Cadmium in Solid Aluminum," *Zh. Neorg. Khim., 9*(6), 1397-1402 (1964) in Russian; TR: *Russ J. Inorg. Chem., 9*(6), 759-762 (1964). (Equi Diagram; Experimental)

65Bur: L.M. Burov and A.A. Yakunin, "Formation of Strongly Supersaturated Solid Solutions in Aluminum-Manganese and Aluminum-Chromium Alloys," *Zh. Fiz. Chem., 39*(8), 1927-1931 (1965) in Russian; TR: *Russ. J. Phys. Chem., 39*(8), 1022-1024 (1965). (Meta Phases; Experimental)

65Ern: D. Ernst, J. Tydings, and M. Pasnak, "Effect of High Pressure on the Al-Mn Binary Alloy System between 40 and 100 at.% Mn," *J. Appl. Phys., 36*(3), 1241-1242 (1965). (Meta Phases; Experimental)

67Mag: L.M. Magat, Ya.S. Shur, G.S. Kandaurova, G.M. Makarova, and N.I. Gusel'nikova, "Crystal Structure and Magnetic Properties of the High-Coercivity Alloy Mn-Al," *Fiz. Met. Metalloved., 23*(3), 226-233 (1967) in Russian; TR: *Phys. Met. Metallogr., 23*(3), 32-39 (1967). (Crys Structure; Experimental)

69Mir: I.A. Miroshnichenko and G.A. Sergeev, "Some Features of the Expansion of the Solid Solution Zone in Eutectic and Peritectic Alloys," *Zh. Fiz. Khim., 43*(6), 1571-1572 (1969) in Russian; TR: *Russ. J. Phys. Chem., 39*(8), 873-874 (1969). (Meta Phases; Experimental)

69Sch: R.W. Schonover and G.P. Mohanty, "Some Structural Studies on the AlMn Phase," *Mater. Sci. Eng., 4*, 243-245 (1969). (Crys Structure; Experimental)

70Ble: J. Bletry, "Solid Solutions of Aluminum with Transition Metals of the First Series," *J. Phys. Chem. Solids, 31*, 1263-1272 (1970). (Meta Phases; Experimental)

70Hin: C.P. Hinesley and James G. Morris, "A Method for Producing Rapidly Cooled Liquid-Quenched Metal Samples Suitable for Tensile Testing," *Metall. Trans., 1*, 1476-1478 (1970). (Meta Phases; Experimental)

71Abr: N.Kh. Abrikosov, L. Ivanova, and V.A. Danil'chenko, "Phase Transition of Mn_4Al_{11} to $MnAl_3$," *Izv. Akad. Nauk SSSR, Neorg. Mater., 7*(6), 1053-1055 (1971) in Russian; TR: *Inorg. Mater., 7*(6), 933-935 (1971). (Equi Diagram, Crys Structure; Experimental)

*71God: T. Godecke and W. Koster, "A Supplement to the Constitution of the Aluminum-Manganese System," *Z. Metallkd., 62*(10), 727-732 (1971) in German. (Equi Diagram; Experimental)

71Yos: K. Yoshida and S. Nagata, "On the Crystal Structure of MnAl(r) Phase," *Jpn. J. Appl. Phys., 10*(1), 7-10 (1971). (Crys Structure; Experimental)

72Bat: G.I. Batalin, E.A. Beloboradova, B.A. Stukalo, and A.A. Chekhovskii, "Thermodynamic Properties of Molten Alloys of Aluminum with Manganese," *Ukr. Khim. Zh., 38*(8), 825-827 (1972) in Russian; TR: *Sov. Prog. Chem., 38*, 83-84 (1972). (Thermo; Experimental)

72Nes: E. Nes, S.E. Naess, and R. Hoier, "Decomposition of an Aluminum-Manganese Alloy," *Z. Metallkd., 63*, 248-252 (1972). (Meta Phases; Experimental)

72Yos: K. Yoshida, "One-Dimensionally Disordered (Mn-Al) Structure in Vacuum Co-Deposited Film," *J. Phys. Soc. Jpn., 32*(2), 431-440 (1972). (Crys Structure; Experimental)

***73Esi:** Yu.O. Esin, N.T. Bobrov, M.S. Petrushevskii, and P.V. Gel'd, "Concentration Variation of the Enthalpies of Formation of Manganese-Aluminum Melts at 1626 K," *Zh. Fiz. Khim., 47*(8), 1959-1962 (1973) in Russian; TR: *Russ. J. Phys. Chem., 47*(8), 1103-1105 (1973). (Thermo; Experimental)

73Hoi: R. Hoier, S.E. Naess, E. Nes, "High-Temperature Decomposition of an $Al_{1.8}Mn$ Alloy," *Z. Metallkd., 64*(9), 640-642 (1973). (Meta Phases, Experimental)

73Vin: E.Z. Vintaikin, V.A. Udovenko, N.N. Luarsabishvili, and L.F. Litvin, "New Ordered Phase in the MnAl Alloy System," *Dokl. Akad. Nauk SSSR, 210*, 1327-1328 (1973) in Russian; TR: *Sov. Phys. Dokl., 18*(6), 432-433 (1973). (Meta Phases; Experimental)

73Yos: K. Yoshida, "Intensity Equation for X-Rays Diffracted by One-Dimensionally Disordered Crystal of δ(Mn-Al)," *J. Phys. Soc. Jpn., 35*(2), 482-488 (1973). (Crys Structure; Experimental)

74Goe: D.B. Goel, U.P. Roorkee, P. Furrer, and H. Warlimont, "Precipitation in Aluminum-Manganese - (Copper-Iron) Alloys," *Aluminium, 50*, 511-516 (1974). (Meta Phases; Experimental)

75Oni: T. Onishi and Y. Nakatani, "Crystal Structures of $MnAl_6$ and $MnAl_4$," *J. Jpn. Inst. Light Met., 25*(7), 253-258 (1975) in Japanese. (Crys Structure; Experimental)

80Kon: A. Kontio, E.D. Stevens, and P. Coppens, "New Investigations of the Structure of Mn_4Al_{11}," *Acta Crystallogr. B, 36*, 435-436 (1980). (Crys Structure; Experimental)

84Fie: R.D. Field and H.L. Fraser, "Precipitates Possessing Icosahedral Symmetry in a Rapidly Solidified Al-Mn Alloy," *Mater. Sci. Eng. 68*, L17-L21 (1984). (Meta Phases; Experimental)

84She1: D. Shechtman, R.J. Schaefer, and F.S. Biancaniello, "Precipitation in Rapidly Solidified Al-Mn Alloys," *Metall. Trans. A, 15*, 1987-1997 (1984). (Meta Phases; Experimental)

***84She2:** D. Shechtman, I. Blech, D. Gratias, and J.W. Cahn, "Metallic Phase with Long-Range Orientational Order and No Translational Symmetry," *Phys. Rev. Lett., 53*(20), 1951-1953 (1984). (Meta Phases; Experimental)

85Ben: L. Bendersky, R.J. Schaefer, F.S. Biancaniello, W.J. Boettinger, M.J. Kaufman, and D. Shechtman, "Icosahedral Al-Mn and Related Phases: Resemblance in Structure," *Scr. Metall., 19*, 909-914 (1985). (Meta Phases; Experimental)

85Des: P. Desai, "Thermodynamic Properties of Binary Al-Mn Alloy System," CINDAS Report (1985). (Thermo; Experimental)

85Guy: P. Guyot and M. Audier, "A Quasicrystal Structure Model for Al-Mn," *Philos. Mag., 52*(1), L15-L19 (1985). (Meta Phases; Experimental)

85Kel: K.F. Kelton and T.W. Wu, "Density Measurements, Calorimetry, and Transmission Electron Microscopy of Icosahedral $Mn_{14}Al_{86}$," *Appl. Phys. Lett., 46*, 1059 (1985). (Meta Phases; Experimental)

85Kim: K. Kimura, T. Hashimoto, K. Suzuki, K. Nagayama, H. Ino, and S. Takeuchi, "Stoichiometry of Quasicrystalline Al-Mn," *J. Phys. Soc. Jpn., 54*, 3217-3219 (1985). (Meta Phases; Experimental)

85Por: R. Portier, D. Shechtman, D. Gratias, and J. Cahn, "High Resolution Electron Microscopy of the Icosahedral Quasiperiodic Structure in Aluminum-Manganese System," *J. Microsc. Spectrosc. Electron., 10*(2), 107-116 (1985). (Meta Phases; Experimental)

86Ben: L. Bendersky, "Quasicrystals with 1*D* Translational Symmetry and a Tenfold Rotation Axis," Proc. Conf. Boston, MA, Dec 1985, in *Rapidly Solidified Alloys and Their Mechanical and Magnetic Properties*, Materials Research Society, Pittsburgh, 237-240 (1986). (Meta Phases; Experimental)

86Sch: R.J. Schaefer, L.A. Bendersky, D. Shechtman, W.J. Boettinger, and F.S. Biancaniello, "Icosahedral and Decagonal Phase Formation in Al-Mn Alloys," *Metall. Trans. A, 17*, 2117-2125 (1986). (Meta Phases; Experimental)

87Mca: A.J. McAlister, L.A. Bendersky, R.J. Schaefer, and F.S. Biancaniello, *Scr. Metall., 21*, 103-106 (1987). (Meta Phases; Experimental)

87Mur: J.L. Murray, A.J. McAlister, R.J. Schaefer, L.A. Bendersky, F. Biancaniello, and D.L. Moffat, *Metall. Trans. A, 18*, 385-392 (1987). (Equi Diagram, Meta Phases; Experimental)

*Indicates key paper.
#Indicates presence of a phase diagram.

Al-Mn evaluation contributed by **A.J. McAlister** and **J.L. Murray**, Center for Materials Science, National Bureau of Standards. This work was jointly funded by the Defense Advanced Research Project Agency (DARPA) and the National Bureau of Standards through the Metallurgy Division and through the Office of Standard Reference Data. Literature searched through 1985. Dr. McAlister and Dr. Murray are the ASM/NBS Data Program Co-Category Editors for binary aluminum alloys.

The B-V (Boron-Vanadium) System

10.811 50.9415

By K.E. Spear and P.K. Liao
Pennsylvania State University

and

J.F. Smith
Ames Laboratory-USDOE
Iowa State University

Equilibrium Diagram

The assessed V-B phase diagram is shown in Fig. 1, and its invariant equilibria are summarized in Table 1. The experimental phase equilibria data used in constructing this diagram are taken primarily from [66Rud]. The liquidus of the assessed diagram was calculated from Gibbs energy functions optimized with respect to thermochemical and phase diagram data.

The equilibrium solid phases of the system are: (1) the terminal solid solutions bcc (V) and rhombohedral (βB); and (2) the intermediate compounds V_3B_2, VB, V_5B_6, V_3B_4, V_2B_3, and VB_2.